

2005

Magnetopolaron interactions in n-type indium phosphide

R. A. Lewis

University of Wollongong, roger@uow.edu.au

P. E. Simmonds

University of Wollongong, simmonds@uow.edu.au

Y. J. Wang

Florida State University, USA

Publication Details

This article was originally published as: Lewis, RA, Simmonds, PE & Wang, YJ, Magnetopolaron interactions in n-type indium phosphide, *Physical Review B*, 2005, 72, 245207. Copyright 2005 American Physical Society. The original journal can be found [here](#).

Magnetopolaron interactions in *n*-type indium phosphide

R. A. Lewis and P. E. Simmonds

Institute for Superconducting and Electronic Materials, University of Wollongong, Wollongong NSW 2522, Australia

Y.-J. Wang

National High Magnetic Field Laboratory at Florida State University, Tallahassee, Florida 32310, USA
(Received 24 December 2004; revised manuscript received 26 August 2005; published 28 December 2005)

Broadband far-infrared absorption spectroscopy is used to investigate *n*-type indium phosphide in magnetic fields of up to 30 T. The large energy range (≈ 2 –14 Ry) and the large magnetic field range ($0 \leq \gamma < 3$) employed permit the observation of a rich variety of magnetopolaron interactions. We report on the magnetopolaron effect for bound states in InP, beginning with the coupling of the $2p_+$ state with the $1s$ +LO phonon state. We further observe the magnetopolaron effect associated with the metastable state (210). In addition we report (i) the re-emergence of the (210) impurity state transition beyond the LO phonon manifold, (ii) the possible coupling of an impurity transition with the $1s$ +2LO phonon state, and (iii) both low- and high-energy one-phonon transitions of impressive richness and detail.

DOI: [10.1103/PhysRevB.72.245207](https://doi.org/10.1103/PhysRevB.72.245207)

PACS number(s): 78.30.-j, 63.20.Dj

I. INTRODUCTION

InP is a direct-gap III-V semiconductor alloy of technological importance in photonics, electronics, and radiation detection. The energy states of bound electrons in InP have been measured by far-infrared spectroscopy^{1–3} and by far-infrared laser magnetospectroscopy^{2,4,5} up to fields of 10 T. The data are well accounted for by the hydrogenic model—the band is largely parabolic and isotropic and central-cell corrections are small. Suzuki *et al.*^{6,7} have reported oscillatory behavior in the absorption spectrum of bulk *n*-InP using laser magnetospectroscopy. A single set of experiments have examined InP in extremely high fields, to 150 T.^{8,9} The data under such challenging experimental conditions are naturally limited, but reveal a magnetopolaron effect.

The present experiments concentrate on the little-explored range of magnetic fields 10–30 T, often with better resolution and better signal-to-noise than enjoyed in earlier work. In particular, the present experiments probe closely the region in which impurity magnetopolaron effects are most prominent. Magnetopolaron interactions have previously been studied in InSb,¹⁰ CdTe,¹¹ and GaAs,¹² but additional features are revealed in this detailed study of magnetopolaron effects associated with bound states in InP.

The unperturbed energy levels of a donor in InP closely match the energy levels of atomic hydrogen scaled by the factors of the electron effective mass m^* and the static dielectric constant of the lattice $\epsilon(0)$ with an effective rydberg

$$\text{Ry}^* = \frac{m^*}{m_e} \frac{1}{\epsilon(0)^2} \text{Ry}. \quad (1)$$

For $\epsilon(0)$ we adopt Meiners' value¹³ of 11.77. For the effective mass we adopt¹⁴ $m^*/m_e = 0.079$ – 0.27 . These values of m^* and $\epsilon(0)$ give the energy scale $\text{Ry}^* = 62.79 \text{ cm}^{-1}$.

In a magnetic field the degeneracy of the impurity energy states is lifted, analogously to the Zeeman effect in atomic hydrogen. A dimensionless measure of magnetic field is

$$\gamma = \frac{\hbar\omega}{2 \text{Ry}}. \quad (2)$$

At $\gamma=1$, the splitting of an $m=1$ state, which is half the cyclotron energy, equals 1 Ry; equivalently, the Bohr radius is equal to the magnetic length. For the chosen values of m^* and $\epsilon(0)$, $\gamma=1$ corresponds to 10.66 T.

We distinguish stable states, which emerge from zero-field atomic states and evolve with field into states associated with Landau states, and metastable states, which evolve from the Landau states as the field is reduced, and have no atomic counterpart. For the stable states the tabulation of Makado and McGill¹⁵ is particularly convenient as the energies of a large number of states are given for a large number of magnetic fields. For the metastable states the results of Blom¹⁶ will be used. These are obtained using a basis-expansion method¹⁷ employing a set of high-field basis states. For clarity, in denoting states we give where applicable both (a) the atomic notation conventionally used at low fields and (b) the quantum numbers applicable to high fields in the notation of Simola and Virtamo;¹⁸ for example, $2p_{1-}(0\bar{1}0)$.

II. EXPERIMENT

The samples studied here were bulk InP not intentionally doped. They were wedged to suppress optical interference between the front and back faces. A Bruker Model IFS 113v Fourier-transform infrared spectrometer equipped with a global source and liquid-helium-cooled Si bolometer detector was used to obtain the spectra. Measurements were made in both a 17.5-T superconducting magnet and a 30-T resistive magnet. In both cases the light was conducted to the sample at the field center via a metal light pipe and a condenser cone. The samples were aligned with a $\langle 100 \rangle$ axis parallel to the field. This was also the direction of the (unpolarized) light propagation (Faraday geometry). In this arrangement, $\mathbf{E} \perp \mathbf{B}$.

TABLE I. Polaron parameters for several semiconductors including CdTe (Ref. 11), InSb (Ref. 10), and GaAs (Ref. 12).

	CdTe	InSb	GaAs	InP
LO phonon cm^{-1}	170	197	296	349.5
Ry^*	1.5	42	6.3	5.6
α	0.4	0.025	0.068	0.12

III. RESULTS AND DISCUSSION

A. Polaron effects—Hybridization of the hydrogenic excited states

At high magnetic fields the $1s_0(000) \rightarrow 2p_{1+}(110)$ transition may be seen to be bending over as its energy approaches the phonon region—the onset of the magnetopolaron effect. Polaron Zeeman effects have been studied in a variety of semiconductors such as InSb,¹⁰ CdTe,¹¹ and GaAs.¹² Among other things the ease of observation depends on the absolute and relative (to hydrogen) energies and magnetic fields at which two levels would cross in the absence of coupling. Representative values for these are given in Table I. Compared to the other materials, the LO phonon energy in InP

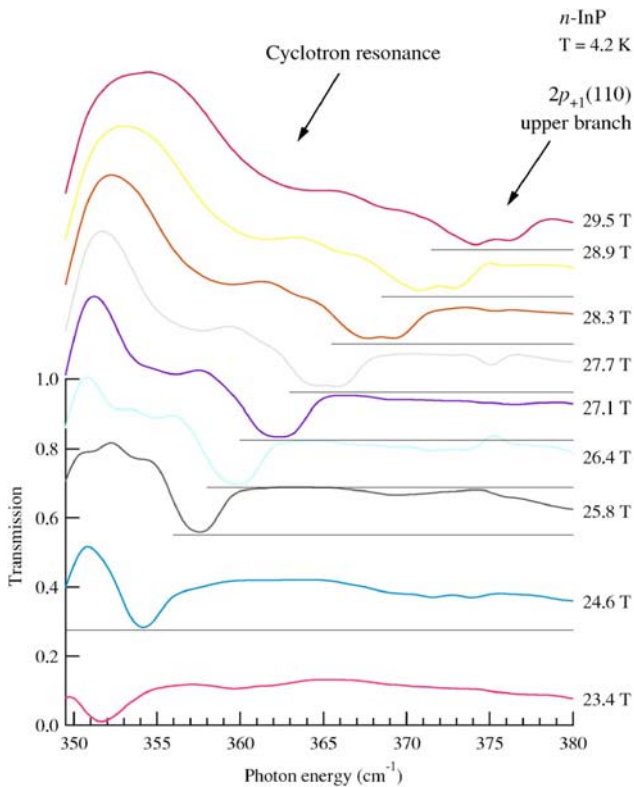


FIG. 1. (Color online) Optical transmission of *n*-InP immediately above the energy of the LO phonon, 349.5 cm^{-1} . The vertical scale applies to each trace when offset by the amount indicated by the zero-transmission line given at each field. The magnetic-field dependence of the two absorption features identified by the arrows is given in Fig. 2.

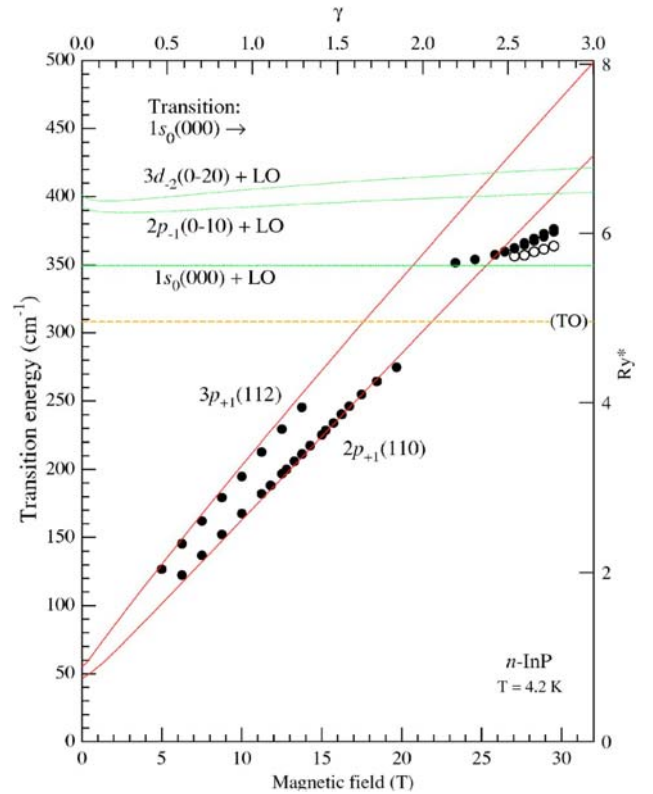


FIG. 2. (Color online) Magnetopolaron coupling in *n*-InP. The $|2p_{1+}(110), 0\text{-phonon}\rangle$ state interacts with the $|1s_0(000), 1\text{-phonon}\rangle$ state. The open circles indicate cyclotron resonance. The $|3p_{1+}(112), 0\text{-phonon}\rangle$ transition is also shown.

when expressed in effective rydbergs is close to that of GaAs, but the coupling constant α is almost twice as large.

The energy of the TO phonon is $308.2 \pm 0.3 \text{ cm}^{-1}$ at 4.2 K.¹⁹ Between this energy and that of the LO phonon, which is $349.5 \pm 0.3 \text{ cm}^{-1}$ at 4.2 K,¹⁹ the sample reflectivity is very high (“reststrahlen region”) and so transmission experiments are impossible. Beyond the reststrahlen region we again detect the hydrogenic transitions, but they are now strongly distorted by interactions involving the LO phonon. Figure 1 shows the transmission of the sample above the LO phonon energy at the highest magnetic fields employed. The energy axis in Fig. 1 starts at the LO-phonon energy. As the magnetic field increases, so does the sample transmission immediately above the LO-phonon energy. The effect is explained in part by the emergence of the feature to be described now. A strong absorption feature is seen starting at 352 cm^{-1} at 23.4 T and increasing in energy with field to end up at $\sim 374 \text{ cm}^{-1}$ at 29.5 T. This is the “classic” magnetopolaron effect that appears as the field is increased to the point where the $1s_0(000) \rightarrow 2p_{1+}(110)$ transition would (in the absence of coupling) coincide with the energy of the LO phonon. We will denote this as the $|2p_{1+}(110), 0\text{-phonon}\rangle$ state crossing the $|1s_0(000), 1\text{-phonon}\rangle$ state, where the phonon involved is understood to be the LO phonon. In the system under study this occurs at a field $\sim 25 \text{ T}$, close to the field limit of the experiment, and so, in contrast to experiments in InSb, CdTe, and GaAs, the full development of this interac-

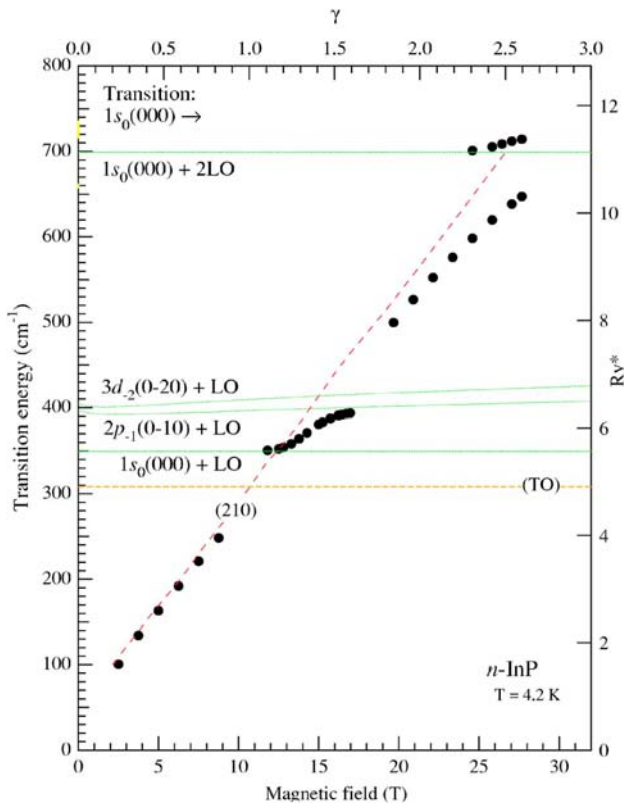


FIG. 3. (Color online) Magnetopolaron coupling of *n*-InP $|(210), 0\text{-phonon}\rangle$ state. The region $715\text{--}735\text{ cm}^{-1}$ is inaccessible to the spectrometer.

tion cannot be followed. The emergence of the state hybridized from the $|2p_{1+}(110), 0\text{-phonon}\rangle$ state and the $|1s_0(000), 1\text{-phonon}\rangle$ state above the LO energy is evident in Fig. 1 and the position as a function of field is given in Fig. 2.

Compared to the situation where the two interacting states are widely separated from other states^{10,11} the hybrid state appears depressed in energy, but this effect is just as observed in the more analogous system of GaAs,¹² where additional states lie close by. The $|1s_0(000), 1\text{-phonon}\rangle$ state first hybridizes with the $|2p_{1+}(110), 0\text{-phonon}\rangle$ state but does not have the opportunity to fully take on the character of the latter because of the proximity of the $|2p_{1-}(0\bar{1}0), 1\text{-phonon}\rangle$ state, also shown in Fig. 2, which it will end up tracking (but beyond the field range of the present experiments). The complete interaction involves repulsion from higher states as well, the next nearest of which is indicated in Fig. 2, the $|3d_{2-}(0\bar{2}0), 1\text{-phonon}\rangle$ state, resulting in further depression compared to an isolated interaction. Similar interactions with a manifold of higher-lying states have been previously observed in quantum wells.^{20,21} At the highest fields this absorption feature is observed to split. This may be due to the central-cell effect, the sample containing at least two donor species.

In Fig. 1, apart from the strong absorption already described, a weaker absorption feature is observed systematically at lower energy. No features related to bound states are expected here. We suggest that this weak feature is cyclotron

absorption, strongly affected by the polaron effect. The previous work in megagauss fields⁸ includes one datum in this region, for $28\ \mu\text{m}=357\text{ cm}^{-1}$ stated to be at 23 T, but the absorption is very broad, with half width of about 20 T. On examining Fig. 4 of Ref. 8 it is quite feasible that the position of the resonance observed is at 26 T, which would correspond with the feature observed here.

In addition to the $|2p_{1+}(110), 0\text{-phonon}\rangle$ transition, Fig. 2 also shows the next higher energy transition, with final state $|3p_{1+}(112), 0\text{-phonon}\rangle$. This is also expected to undergo a polaron interaction with the $|1s_0(000), 1\text{-phonon}\rangle$ state, as well as with other states of higher energy. Such interactions are weak and difficult to identify (see Fig. 1) and not discerned well enough to show in Fig. 2.

Figure 3 shows next higher energy transition, with the metastable state $|(210), 0\text{-phonon}\rangle$ undergoing multiple polaron interactions. A polaron interaction involving a meta-

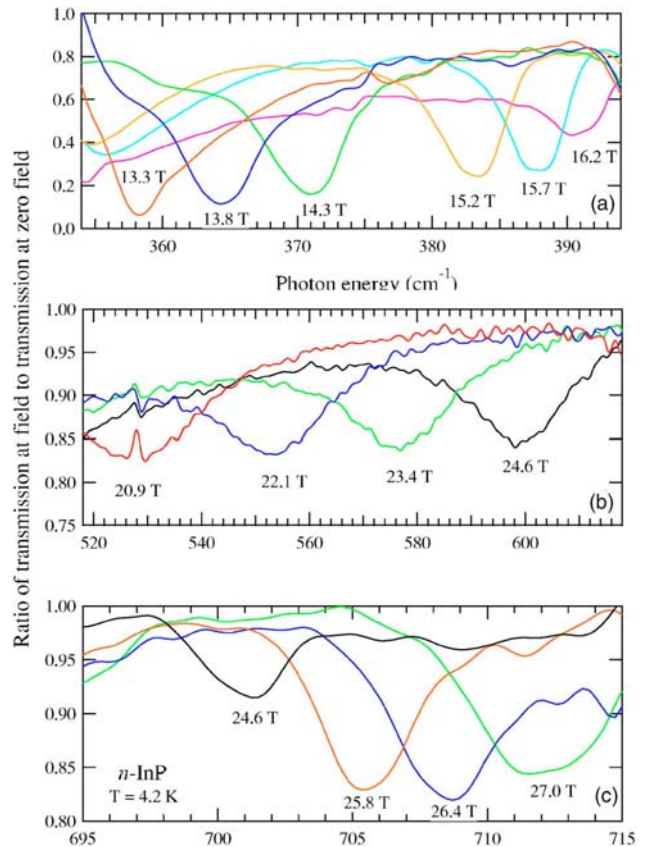


FIG. 4. (Color online) High-energy and high-field features observed in the far-infrared transmission spectrum of *n*-InP. The spectra at field have been ratioed with the spectrum at zero field to reduce field-independent transmission variations. The spectra in the middle panel have a lower signal-to-noise ratio than those in the top and bottom panels because the transmission is less in this region. (a) Region in which the $|(210), 0\text{-phonon}\rangle$ state interacts with $|1s_0(000), 1\text{-phonon}\rangle$ state then with the $|2p_{1-}(0\bar{1}0), 1\text{-phonon}\rangle$ state (see Fig. 3 also). (b) Region in which the $|(210), 0\text{-phonon}\rangle$ state returns to its original trajectory (see Fig. 3 also). (c) Emergence at high field of a possible $|(210), 0\text{-phonon}\rangle, |1s_0(000), 2\text{-phonon}\rangle$ interaction.

stable state, (310) , has been reported previously in a semiconductor system,²² over a very limited field range. As for the $|2p_{+1}(110), 0\text{-phonon}\rangle$ state shown in Figs. 1 and 2, this final state first interacts with the $|1s_0(000), 1\text{-phonon}\rangle$ state. This then gives way to a hybridization with the $|2p_{-1}(0\bar{1}0), 1\text{-phonon}\rangle$ state. In Fig. 4(a) spectra are presented in the field range where these interactions occur, 13–17 T. As the magnetic field is increased, further hybridization is expected involving the $|3d_{-2}(0\bar{2}0), 1\text{-phonon}\rangle$ and higher states; such interactions are difficult to discern in the spectra. At higher fields still, far from the low-energy hydrogenic states compounded with the LO phonon, a $|1s_0(000), 0\text{-phonon}\rangle \rightarrow |(210), 0\text{-phonon}\rangle$ transition is seen close to the unperturbed hydrogenic trajectory. Figure 4(b) shows spectra in this region, in the field range 20–25 T. Around 25 T, the trajectory is seen to bend again. This is attributed to another polaronic interaction—either with the higher-energy states discussed in Sec. III C, or possibly with the 2-LO phonon at energy 699 cm^{-1} , indicated in Fig. 3.

At higher fields still a distinct and unusual feature emerges. This is shown in Fig. 4(c), in which spectra are given in the field range 24–27 T. This clear absorption line abruptly appears at 25 T. Such a sudden appearance is characteristic of hybridization involving a virtual state, as, for example, the transition just described and displayed in Fig. 4(b), and the transition shown in Fig. 2 of Ref. 12. The line is observed for five magnetic fields before moving in energy to beyond the high-energy limit of the spectrometer. Further measurements with a mid-infrared apparatus, and at high

field ($>28\text{ T}$), are necessary to unambiguously determine the origin of this distinctive absorption line, but we suggest, on the basis of the energy and the energy dependence on magnetic field, that it is associated with the the upper branch of the $|(210), 0\text{-phonon}\rangle$ state interacting with the $|1s_0(000), 2\text{-phonon}\rangle$ state.

B. Polaron effects—Low-energy one-phonon states

A large number of absorption features that appear in the energy region immediately above the reststrahlen band were omitted from Figs. 2 and 3 for reasons of clarity. These are shown in detail in Fig. 5. These are transitions from the ground state to, in order of increasing energy, the $|2p_{-1}(0\bar{1}0), 1\text{-phonon}\rangle$, $|3d_{-2}(0\bar{2}0), 1\text{-phonon}\rangle$, and $|4f_{-3}(0\bar{3}0), 1\text{-phonon}\rangle$ states. A similar observation has been made by Cheng *et al.* in GaAs.¹² A splitting of the states that increases with field is observed and is attributed to the central-cell effect. Such splitting was not observed by Cheng *et al.*¹² From the work in GaAs,¹² we might expect to see one state hybridize through the 0-phonon transitions (the theoretical energies of these are also shown in the figure) into the next higher state as field increases. While there is some suggestion of this we do not observe it unequivocally in our data. This is understandable in that there are numerous weak features (many of which are split, complicating matters), closely spaced, through which the 0-phonon transitions move very rapidly with field.

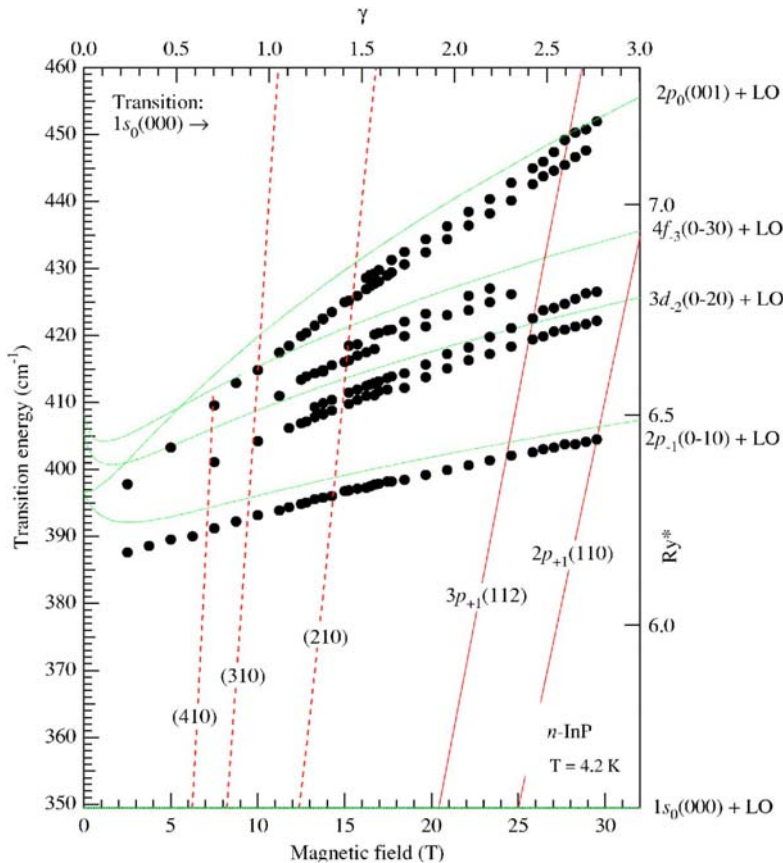


FIG. 5. (Color online) Transitions to low-energy one-phonon states.

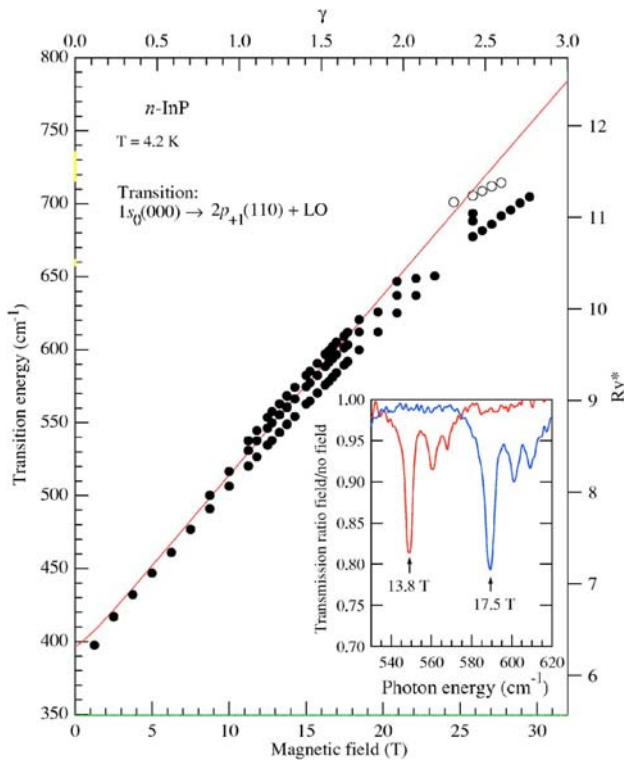


FIG. 6. (Color online) Transitions to high-energy one-phonon states. Open circles are the transition shown in Fig. 4(c). Inset shows the main feature and its two satellites at two magnetic fields. The region $715\text{--}735\text{ cm}^{-1}$ is inaccessible to the spectrometer.

C. Polaron effects—High-energy one-phonon states

A very strong absorption is observed at energies corresponding to the transition from the ground state to the $|2p_{+1}(110), 1\text{-phonon}\rangle$ state (Fig. 6). The strong absorption is

accompanied by two, successively weaker, higher-energy satellites (inset, Fig. 6). The phenomenon cannot be a hydrogenic donor with huge central-cell shift or a multiply ionized donor. The strongest absorption may be regarded as a “phonon replica” of the $|2p_{+1}(110), 0\text{-phonon}\rangle$ transition, however, the energy difference is always less than the phonon energy and decreases systematically with field. Moreover, the two higher-energy satellites are not replicas of transitions observed at low energies, but rather differ by the cyclotron energy from the $|1s_0(000), 0\text{-phonon}\rangle \rightarrow |3d_{-2}(0\bar{2}0), 1\text{-phonon}\rangle$, and $|1s_0(000), 0\text{-phonon}\rangle \rightarrow |4f_{-3}(0\bar{3}0), 1\text{-phonon}\rangle$ transitions, respectively.

IV. CONCLUSION

We report many magnetopolaron interactions of bound states in *n*-InP. The $|2p_{+1}(110), 0\text{-phonon}\rangle$ state couples with the $|1s_0(000), 1\text{-phonon}\rangle$ state as shown in Fig. 2. A splitting of this interaction has been resolved, possibly due to the central-cell effect. Our observations of the evolution of the metastable state (210) with field (Fig. 3) reveal several interesting phenomena: the re-emergence of the original transition beyond the one-phonon manifold and a possible magnetopolaron interaction involving the two-phonon manifold. The richness of detail observed for the one-phonon states of both low energy (Fig. 5) and high energy (Fig. 6) will provide a stringent testing ground for theories that attempt to model such transitions.

ACKNOWLEDGMENTS

This work was supported by the Australian Research Council and the University of Wollongong. Part of the work was performed at the National High Magnetic Field Laboratory, which is supported by NSF Cooperative Agreement No. DMR-9527035 and by the State of Florida.

- ¹J. M. Chamberlain, H. B. Ergun, K. A. Gehring, and R. A. Stradling, *Solid State Commun.* **9**, 1563 (1971).
- ²K. M. Lau and W. L. Wilson, Jr., *Infrared Phys.* **12**, 311 (1983).
- ³N. Iwata and T. Inoshita, *Appl. Phys. Lett.* **50**, 1361 (1987).
- ⁴M. S. Skolnick, P. J. Dean, L. L. Taylor, D. A. Anderson, S. P. Najda, C. J. Armistead, and R. A. Stradling, *Appl. Phys. Lett.* **44**, 881 (1984).
- ⁵C. J. Armistead, P. Knowles, S. P. Najda, and R. A. Stradling, *J. Phys. C* **17**, 6415 (1984).
- ⁶M. Suzuki, H. Kobori, and T. Ohyama, *Physica B* **298**, 203 (2001).
- ⁷M. Suzuki, H. Kobori, and T. Ohyama, *J. Phys. Soc. Jpn.* **72**, 1127 (2003).
- ⁸S. P. Najda, H. Yokoi, S. Takeyama, N. Miura, and P. Pfeffer, *Phys. Rev. B* **44**, 1087 (1991).
- ⁹W. Zawadzki, P. Pfeffer, S. P. Najda, H. Yokoi, S. Takeyama, and N. Miura, *Phys. Rev. B* **49**, 1705 (1994).
- ¹⁰E. J. Johnson and D. M. Larsen, *Phys. Rev. Lett.* **16**, 655 (1966).
- ¹¹D. R. Cohn, D. M. Larsen, and B. Lax, *Phys. Rev. B* **6**, 1367 (1972).
- ¹²J.-P. Cheng, B. D. McCombe, J. M. Shi, F. M. Peeters, and J. T. Devreese, *Phys. Rev. B* **48**, 7910 (1993).
- ¹³L. G. Meiners, *J. Appl. Phys.* **59**, 1611 (1986).
- ¹⁴M. A. Hopkins, R. J. Nicholas, P. Pfeffer, W. Zawadzki, D. Gauthier, J. C. Portal, and M. A. DiForte-Poisson, *Semicond. Sci. Technol.* **2**, 568 (1987).
- ¹⁵P. C. Makado and N. C. McGill, *J. Phys. C* **19**, 873 (1986).
- ¹⁶A. Blom (private communication).
- ¹⁷K. Nilsson, A. Blom, and V. V. Shlyapin, *Solid State Commun.* **132**, 187 (2004).
- ¹⁸J. Simola and J. Virtamo, *J. Phys. C* **11**, 3309 (1978).
- ¹⁹A. Mooradian and G. B. Wright, *Solid State Commun.* **4**, 431 (1966).
- ²⁰P. E. Simmonds, M. S. Skolnick, T. A. Fisher, K. J. Nash, and R. S. Smith, *Phys. Rev. B* **45**, 9497 (1992).
- ²¹L. Świerkowski, J. Szymański, P. E. Simmonds, T. A. Fisher, and M. S. Skolnick, *Phys. Rev. B* **51**, 9830 (1995).
- ²²X. H. Shi, P. L. Liu, G. L. Shi, C. M. Hu, Z. H. Chen, S. C. Shen, J. X. Chen, H. P. Xin, and A. Z. Li, *Appl. Phys. Lett.* **72**, 1487 (1998).